

Home Search Collections Journals About Contact us My IOPscience

The photoluminescence and magnetism of nitrogen-implanted ZnO

This article has been downloaded from IOPscience. Please scroll down to see the full text article.

2011 Phys. Scr. 83 045704

(http://iopscience.iop.org/1402-4896/83/4/045704)

View the table of contents for this issue, or go to the journal homepage for more

Download details:

IP Address: 141.213.168.84

The article was downloaded on 24/04/2011 at 01:39

Please note that terms and conditions apply.

doi:10.1088/0031-8949/83/04/045704

The photoluminescence and magnetism of nitrogen-implanted ZnO

CM Liu¹, X Xiang¹, Y Zhang², HQ Gu¹, Y Jiang¹, M Chen¹ and XT Zu¹

- ¹ Department of Applied Physics, University of Electronic Science and Technology of China, Chengdu 610054, People's Republic of China
- ² School of Physics, Peking University, Beijing 100871, People's Republic of China

E-mail: cmliu@uestc.edu.cn and cmliu028@163.com

Received 30 October 2010 Accepted for publication 7 March 2011 Published 22 March 2011 Online at stacks.iop.org/PhysScr/83/045704

Abstract

Single crystal ZnO was implanted using nitrogen ions with an energy of 60 keV. The microstructure, photoluminescence (PL) and magnetism were studied in detail. Except for nitrogen, no other impurity can be detected by x-ray photoelectron spectra measurements. The room temperature PL of pure ZnO consists of a weak ultraviolet (UV) emission band and a strong green emission band. The PL and electrical conductivity can be suppressed by nitrogen implantation or by annealing in air. However, the two emission bands of pure ZnO can be enhanced intensively by Ar⁺ etching. The PL is related to the structure defects. Moreover, the intensity of UV luminescence is likely correlated to the electrical conductivity. Ferromagnetism cannot be obtained in the nitrogen-implanted sample from 77 to 300 K. The absence of ferromagnetism in nitrogen-implanted ZnO may be because there is no strong interaction between N 2p and O 2p electrons as nitrogen is a deep acceptor in ZnO.

PACS numbers: 78.55.Et, 75.50.Pp

1. Introduction

The magnetism of ZnO free of magnetic transition metal was widely studied because of its potential application as a diluted magnetic semiconductor [1–13]. Up to now, room temperature ferromagnetism has been obtained experimentally in various systems of ZnO material, such as pure ZnO films [1], pure ZnO nanoparticles [2], Ar-implanted ZnO single crystal [3], $Zn_x(ZnO)_{1-x}$ granular films [4], carbon-doped ZnO films [5–7], nitrogen-doped ZnO films [8] and carbon and nitrogen dual-doped ZnO powders [9, 10]. The origin of magnetism was widely attributed to intrinsic defects (oxygen vacancy [2] and zinc interstitials [1, 4]) or light no-metal dopants (carbon and nitrogen [5–7], [9, 10]). Taking into account the stability and reproducibility, the light no-metal dopants seem to be more preferable than the intrinsic defects [11].

Nitrogen is an interesting dopant for ZnO. Its ionic radius is nearly the same as that of oxygen. Although ferromagnetism has been obtained in nitrogen-doped ZnO by calculation [12, 13] and experiment [8], there is still some debate. For example, the calculation attributed the main magnetism to the spin-polarized 2p electrons of nitrogen dopants [12, 13]. However, the magnetism was experimentally

interpreted using the bound magnetic polaron resulting from the net spin in the d-orbits of Zn [8]. There is also the argument about the carriers' type (electron or hole) in mediating the magnetic interaction [5, 9]. In addition, no agreement is obtained about the role of nitrogen impurity in the magnetism of carbon-doped ZnO [9, 10]. Therefore, more work is needed to better understand the mechanism of magnetism in nitrogen-doped ZnO.

Besides the magnetism, the photoluminescence (PL) and electrical conductivity of nitrogen-doped ZnO were also intensively investigated [14–21]. Recently reported results [21] indicate that nitrogen dopant cannot induce p-type conductivity in ZnO as it is a deep acceptor in ZnO. The faults of previous calculations are that they are based on density functional theory (DFT) with local density approximation or generalized gradient approximation (GGA) [21]. It should be noted that the theory-predicted ferromagnetism in nitrogen-doped ZnO is also based on DFT with GGA [12, 13]. Therefore, it is necessary to reconsider the PL, electrical conductivity and magnetism of nitrogen-doped ZnO. We study the magnetism and optical properties of nitrogen-implanted ZnO single crystal in this paper. Our data can be interpreted using the calculation results [21].

1

Phys. Scr. **83** (2011) 045704

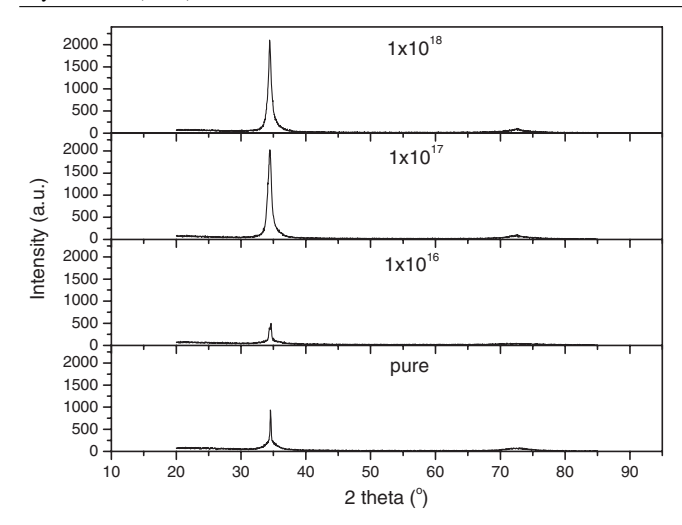


Figure 1. XRD patterns of pure ZnO and nitrogen-implanted samples.

2. Experiments

The nitrogen-doped ZnO samples were fabricated by nitrogen ion implantation using a $10 \times 10 \times 0.5 \,\mathrm{mm}^3$ polished single crystal ZnO substrate with a (0001) crystallographic axis. The single-crystal ZnO substrates were available from Hefei Kejing Materials Technology Co. Ltd. The nitrogen implantation in ZnO was performed at the energy of 60 keV with the nominal dose of 1×10^{16} , 1×10^{17} or 1×10^{18} ions cm⁻² in a vacuum chamber of 2×10^{-3} Pa. The substrate was kept at room temperature by the circulation of cooling water during ion implantation. The crystalline structure of the material was analyzed by x-ray diffraction (XRD) using a Philips X'Pert diffractometer with Cu-K α radiation (= 0.154 056 nm). The samples' stoichiometry was measured by Kratos X SAM 800 x-ray photoelectron spectroscopy (XPS). The absorption spectra of the samples were measured on a Shimadzu UV-2500 UV-visible spectrophotometer. The PL spectra were measured using a Shimadzu RF-5301PC spectrofluorophotometer. The magnetic properties were analyzed using the MPMS XL-7 Magnetic Property Measurement System.

3. Results and discussion

Figure 1 shows the XRD patterns of pure ZnO and nitrogen-implanted samples. Only a strong (002) diffraction peak corresponding to the wurtzite structure is present for all samples. No other impurity phases are detected by XRD measurements. With the nitrogen doping increasing, the peak intensity firstly decreases for 1×10^{16} ions cm⁻² and then increases greatly with doping concentration further increasing. The penetration depth of the x-ray for ZnO is taken as $2 \mu m$ [22], which is much larger than the nitrogen implantation depth (about 210 nm as determined by TRIM96 [23] calculation). So, much of the XRD signal comes from the unimplanted ZnO. The big change in XRD means that nitrogen implantation has a large influence on the unimplanted ZnO. One possible reason of this may be that the energy of implanted ions is transferred to the unimplanted ZnO layer. Yen et al [14] reported that

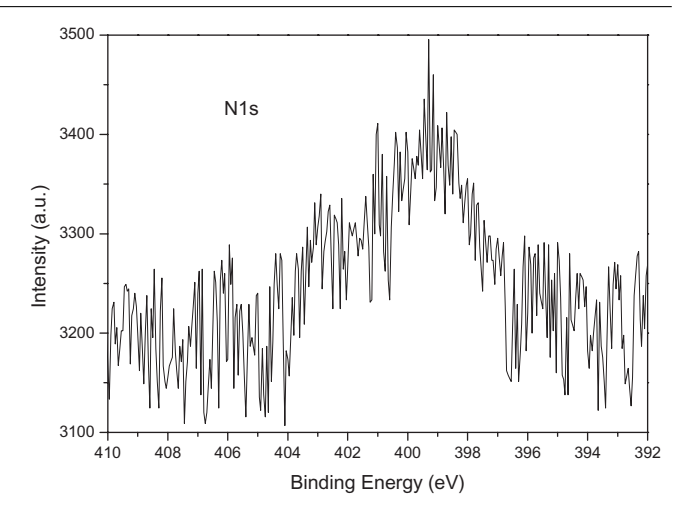


Figure 2. N1s XPS of the 1×10^{18} ions cm⁻² implanted sample.

nitrogen doping provided better crystal quality of ZnO films. However, this is different from the reported results of Wang *et al* [15]. Our results indicate that the structure depends on the doping concentration. The samples are found to change from conducting to insulating by nitrogen implantation. The increase of resistivity by nitrogen doping was attributed to the decrease of carrier concentration and mobility [15]. The deep acceptor level of nitrogen dopants [21] may yield low carrier concentration [16]. Besides, the nitrogen dopants were supposed to create defects, which can capture part of the itinerant electrons [8].

The nitrogen incorporation in ZnO is confirmed by measuring the XPS. Figure 2 indicates the N1s XPS of $1 \times$ 10¹⁸ ions cm⁻² implanted samples. The XPS was measured after the sample was etched about 10 nm. According to the reported results [16, 17], the nitrogen dopant in ZnO has fairly complex chemical states. The N1s signals located at $406\,eV$ [17] and $403-404\,eV$ [16] were assigned to N_2 on the oxygen site. The peaks around 399 eV were assigned to the overlap of the N-H and C-N components [16]. The peak at about 398 eV was attributed to the signal of the N-Zn bond [16, 17]. For our sample, the N1s signal has a broad peak ranging from 404 to 394 eV, with a maximum intensity at about 399 eV. Based on the XPS data, the calculated ratio of N/(N+O+Zn) is about 12.1%, which is similar to that obtained from TRIM96 (11.8%). The nitrogen implantation depth obtained from TRIM96 calculation is about 210 nm. No transition metal impurity (such as Fe, Co and Ni) can be detected in the implanted sample or the pure sample.

Figure 3 illustrates the room temperature PL spectra. As the penetration depth of 325 nm light for ZnO is about 60–120 nm [24], the PL signal of the nitrogen-implanted sample is completely from the nitrogen-implanted layer. As indicated in figure 3, the PL of pure ZnO has two emission bands. There are a weak ultraviolet (UV) emission band and a strong broad green emission band around 373 nm (3.32 eV) and 540 nm (2.30 eV), respectively. The UV band is usually attributed to the near band edge free excitation emission [18]. However, the 3.31 eV emission peak is regarded as related to basal-plane stacking faults [19]. The green emission band is related to defects (such as zinc vacancy [14] and oxygen vacancy [20]). For all three nitrogen-implanted samples, both

Phys. Scr. **83** (2011) 045704

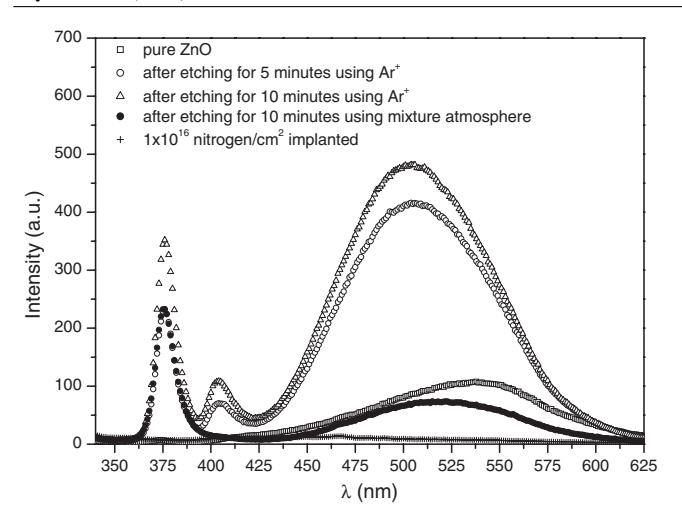


Figure 3. Room temperature PL spectra. The excitation wavelength is 325 nm.

of the UV and green emission bands disappear regardless of whether the XRD diffraction peak is weakened or enhanced. The nitrogen dopant related emission [15] is also not observed in our samples. It was supposed that the nitrogen dopant in the interstitial sites might suppress the luminescence [8]. Wang *et al* also reported that nitrogen dopant in ZnO can greatly reduce the intensity of PL [15]. The recent calculation indicated that nitrogen is a deep acceptor in ZnO with an acceptor level of 1.3 eV [21]. The deep nature of the N acceptor is clearly inconsistent with PL peaks that occur within a few 0.1 eV of the band gap [21].

Annealing and Ar⁺ etching were utilized to understand the origin of PL. The Ar⁺ etching was performed in a vacuum chamber with a base pressure of 1.4×10^{-3} Pa. The working pressure was about 1.0×10^{-2} Pa. Using sputter yield obtained from TRIM96, the etching rate was estimated to be about $0.17 \,\text{Å}\,\text{s}^{-1}$. The sample was kept at room temperature during etching. It is found that annealing in air at various temperatures has no effect on the PL and conductivity of nitrogen-implanted samples. But both the PL and electrical conductivity of the pure sample are quenched by annealing in air at 300 °C for 1 h. Figure 3 shows that the PL intensity of pure ZnO increases greatly after 1 keV Ar+ etching. There is a blue-shift of about 36 nm for the green emission band. The intensity of PL is enhanced when the etching time is increased from 5 to 10 min. Compared to the original pure ZnO single-crystal sample, the UV emission of the Ar⁺ etched sample for 10 min increases about 99 times. The green emission signal increases about 4.5 times. Furthermore, there appears a new emission band located at about 405 nm, which was attributed to the zinc vacancy [25]. This suggests that structure defects can be introduced by Ar⁺ etching. As a result, the structure defects can be controlled by adjusting the etching condition (such as the etching atmosphere, energy of Ar⁺ and base pressure). For example, besides the UV and green luminescence, a new emission peak around 415 nm is obtained after the pure sample is etched in a higher base pressure and energy of 1×10^{-7} Pa and 2 keV (this figure is not shown here). Compared to that etched in pure Ar atmosphere, figure 3 indicates that the emission band around 405 nm is not present after the sample is etched in a mixture

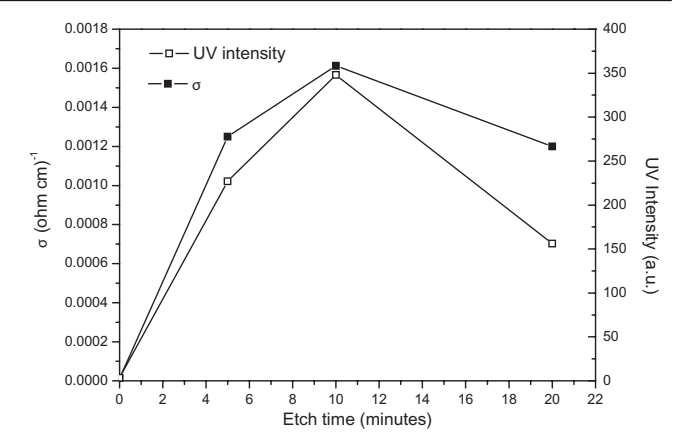


Figure 4. Electrical conductivity and the UV emission intensity as a function of etching time.

atmosphere of nitrogen and argon (the gas flowing ratio of nitrogen to argon is about 3:1). Since the UV emission is increased greatly by Ar⁺ etching, it is likely from the stacking faults [19]. This giant enhancement of UV intensity induced by Ar⁺ etching is useful for optoelectronics. As the 405 nm emission band is not present in the mixture etching atmosphere, the introduction of nitrogen in the etching process can reduce the zinc vacancy. The Ar⁺ etching has no effect on the PL and electrical conductivity of nitrogen-implanted samples.

Figure 4 shows the electrical conductivity and the UV emission intensity of pure ZnO as a function of Ar^+ etching time. The resistivity is decreased from 0.9×10^6 to $0.62 \times 10^3 \,\Omega$ cm by Ar^+ etching for 10 min. It was indicated that the blue light emission of Ar^+ irradiated SrTiO₃ is highly correlated to conductivity [26]. Yu *et al* [27] also reported that the intensity of PL of the ZnO film is proportional to the conductivity. As indicated in figure 4, the PL intensity and conductivity have a similar dependence on the etching time. Thus we think that the UV emission of ZnO is also correlated to the conductivity. The conductivity has a close relationship to structure defects [26]. The absence of luminescence by nitrogen implantation and annealing should have partly resulted from the insulating character.

Figure 5 shows the absorption spectra for the pure sample and nitrogen-implanted samples. For all three nitrogen-implanted samples, there is an evident enhanced absorption in the region from 400 to 500 nm. This enhancement in the absorption may be due to the impurity-induced states in the band gap [28]. Futsuhara *et al* [29] also observed a red-shift of the optical band gap Eg for the N-doped ZnO, which was assigned to the decrease in ionicity caused by the formation of Zn–N bonds.

The room temperature hysteresis was measured for the Ar^+ etched, 1×10^{16} and 1×10^{18} ions cm⁻² implanted samples, respectively. The hysteresis at 77 K was measured for the 1×10^{18} ions cm⁻² implanted sample. Only diamagnetism is detected for these samples. Figure 6 shows the room temperature hysteresis for the 1×10^{18} ions cm⁻² implanted sample. If the magnetism can be regarded as carrier mediated [5, 9, 10, 12], the absence of ferromagnetism in the nitrogen-doped samples may be partly due to the insulating character. It was also reported that nitrogen incorporation into

Phys. Scr. **83** (2011) 045704 C M Liu et al

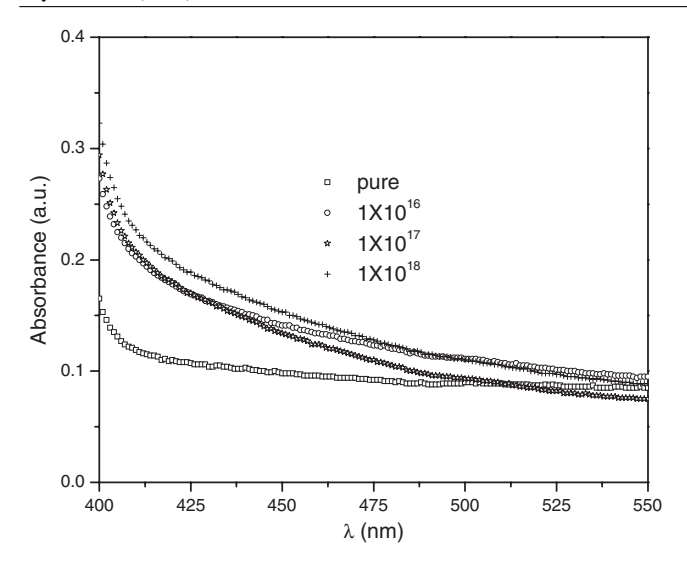


Figure 5. Absorption spectra of the pure sample and nitrogen-implanted sample.

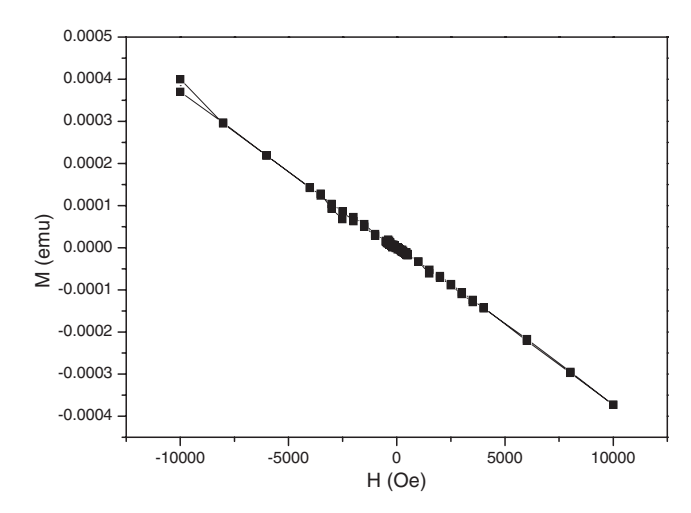


Figure 6. Room temperature hysteresis of the 1×10^{18} ions cm⁻² implanted sample.

carbon-doped ZnO leads to a decrease of electron density, leading to the weakening of ferromagnetic interaction [9]. On the other hand, the spin polarization of N 2p electrons results from the strong interaction between O 2p and N 2p electrons [12]. If the nitrogen is a deep acceptor impurity in ZnO [21], there should be no significant overlap of N 2p and O 2p states, suggesting that there is no strong interaction between them to induce spin polarization of N 2p states in ZnO.

4. Conclusion

In summary, the influence of nitrogen implantation on microstructure, optical properties and magnetism is studied. It is found that nitrogen implantation or annealing in an air atmosphere can suppress the PL and electrical conductivity of ZnO. There is an enhanced absorption in the region from 400 to 500 nm for nitrogen-implanted samples. No ferromagnetism can be obtained in nitrogen-implanted samples from 77 to 300 K. An interesting result is that UV emission of the pure ZnO sample can be greatly increased by etching the sample using Ar⁺ in a vacuum. The UV emission

is likely correlated to the structure defects. The absence of ferromagnetism in nitrogen-implanted ZnO can be interpreted by taking the nitrogen impurity as a deep acceptor in ZnO.

Acknowledgments

This study was supported financially by the National Natural Science Foundation of China (grant no. 10904008) and the Foundation for Young Scholars of the University of Electronic Science and Technology of China (grant no. L08010401JX0806).

References

- [1] Hong N H, Sakai J and Brizé V 2007 J. Phys.: Condens. Matter 19 036219
- [2] Sundaresan A, Bhargavi R, Rangarajan N, Siddesh U and Rao C N R 2006 Phys. Rev. B 74 161306
- [3] Borges R P, da Silva R C, Magalhães S, Cruz M M and Godinho M 2007 J. Phys.: Condens. Matter 19 476207
- [4] Zhang X, Cheng Y H, Li L Y, Liu H, Zuo X, Wen G H, Li L, Zheng R K and Ringer S P 2009 *Phys. Rev.* B **80** 174427
- [5] Pan H, Yi J B, Shen L, Wu R Q, Yang J H, Jin J Y, Feng Y P, Ding J, Van L H and Yin J H 2007 Phys. Rev. Lett. 99 127201
- [6] Zhou S Q et al 2008 Appl. Phys. Lett. 93 232507
- [7] Herng T S, Lau S P, Wang L, Zhao B C, Yu S F, Tanemura M, Akaike A and Teng K S 2009 Appl. Phys. Lett. 95 012505
- [8] Yu C F, Lin T J, Sun S J and Chou H 2007 J. Phys. D: Appl. Phys. 40 6497
- [9] Ye X J, Song H A, Zhong W, Xu M H, Qi X S, Jin C Q, Yang Z X, Au C T and Du Y W 2008 J. Phys. D: Appl. Phys. 41 155005
- [10] Yi J B, Shen L, Pan H, Van L H, Thongmee S, Hu J F, Ma Y W, Ding J and Feng Y P 2009 J. Appl. Phys. 105 07C513
- [11] Bouzerar G and Ziman T 2006 Phys. Rev. Lett. 96 207602
- [12] Shen L, Wu R Q, Pan H, Peng G W, Yang M, Sha Z D and Feng Y P 2008 Phys. Rev. B 78 073306
- [13] Wang Q, Sun Q and Jena P 2009 New J. Phys. 11 063035
- [14] Yen T F, Dinezza M, Haungs A, Kim S J, Anderson W A and Cartwright A N 2009 *J. Vac. Sci. Technol.* B **27** 1943
- [15] Wang Y G, Lau S P, Zhang X H, Lee H W, Hng H H and Tay B K 2003 J. Cryst. Growth 252 265
- [16] Zhang J P, Zhang L D, Zhu L Q, Zhang Y, Liu M, Wang X J and He G 2007 J. Appl. Phys. 102 114903
- [17] Jiao S, Lu Y, Zhang Z, Li B, Yao B, Zhang J, Zhao D, Shen D and Fan X 2007 J. Appl. Phys. 102 113509
- [18] Kumari L and Li W Z 2010 Cryst. Res. Technol. 45 311
- [19] Thonke K, Schirra M, Schneider R, Reiser A, Prinz G M, Feneberg M, Biskupek J, Kaiser U and Sauer R 2009 Microelectron. J. 40 210
- [20] Leiter F H, Alves H R, Hofstaetter A, Hofmann D M and Meyer B K 2001 Phys. Stat. Sol. B 226 R4
- [21] Lyons J L, Janotti A and Van de Walle C G 2009 Appl. Phys. Lett. 95 252105
- [22] Sawai Y, Hazu K and Chichibu S F 2010 J. Appl. Phys. 108 063541
- [23] Ziegler J E, Biersack J P and Littmark U 1985 The Stopping and Range of Ions in Solids ed J E Ziegler (New York: Pergamon)
- [24] Zou C W, Yan X D, Han J, Chen R Q, Bian J M, Haemmerle E and Gao W 2009 Chem. Phys. Lett. 476 84
- [25] Wu X L, Siu G G, Fu C L and Ong H C 2001 Appl. Phys. Lett. 78 2285
- [26] Kan D et al 2005 Nature Mater. 4 816
- [27] Yu C F, Sung C W, Chen S H and Sun S J 2009 Appl. Surf. Sci. 256 792
- [28] Lee J Y, Park J and Cho J H 2005 Appl. Phys. Lett. 87 011904
- [29] Futsuhara M, Yoshioka K and Takai O 1998 Thin Solid Films 317 322